Functional interplay between MYCN, NCYM and OCT4 promotes aggressiveness of human neuroblastomas

（MYCN と NCYM、OCT4 の機能的相互作用は神経芽腫の悪性化を促進する）

千葉大学大学院医学薬学府

先端生命科学専攻

（主任：田川　雅敏教授）

金子　伊樹

Contents

Abstract

De novo gene birth from non-genic DNA has been recently reported as one of the models of new gene generation. However, the mechanisms by which *de novo* evolved proteins modify pre-existing gene regulatory networks to modulate cellular phenotypes remain unknown. We previously showed that *NCYM*, a *MYCN cis*-antisense gene, encodes a *de novo* evolved protein in the taxonomically restricted group including humans. *NCYM* is co-amplified with the *MYCN* gene in primary human neuroblastomas, and the gene product promotes aggressiveness of neuroblastoma via stabilization of MYCN. In this study, we show that *NCYM* forms a positive feedback loop with *OCT4*, a core regulatory gene maintaining a multipotent state of neural stem cells. In 36 *MYCN*-amplified primary human neuroblastomas, *OCT4* mRNA expression was associated with unfavorable prognosis and was correlated with that of *NCYM*. OCT4 induced both *NCYM* and *MYCN* in human neuroblastoma cells whereas NCYM stabilized MYCN to induce *OCT4* and stem cell-related genes, including *NANOG*, *SOX2*, and *LIN28*. In sharp contrast to MYCN, enforced expression of c-MYC did not enhance OCT4 expression in human neuroblastoma cells. All-*trans* retinoic acid (ATRA) treatment reduced MYCN, NCYM, and OCT4 expression, accompanied by the decreased amount of OCT4 recruited onto intron 1 region of MYCN. Knockdown of NCYM or OCT4 inhibited neurosphere formation and promoted asymmetric cell division in *MYCN*-amplified human neuroblastoma cells. These results suggest that the functional interplay between NCYM and OCT4 maintains stem

cell-like state of human neuroblastomas contributing to their aggressiveness and illustrate that a *de novo* evolved gene can regulate cellular phenotypes by the modulation of pre-existing gene regulatory networks.

Introduction

Neuroblastoma is a pediatric solid tumor that arises in sympatho-adrenal tissues (1). Amplification of the *MYCN* oncogene is frequently observed in unfavorable neuroblastomas (2), and aberrant expression of *MYCN* contributes to neuroblastoma progression (3). MYCN is a transcription factor that regulates a wide variety of biological phenomena, including cell-cycle progression, apoptosis, differentiation and stemness (4, 5). *MYCN* transgenic mice spontaneously develop neuroblastomas (3), but unlike human *MYCN*-amplified neuroblastomas, the mice rarely have metastatic tumors. Recently, we reported that *NCYM,* a *MYCN cis*-antisense gene, encodes a protein that functions as an onco-promoting factor (6). The coding sequence of *NCYM* is not evolutionally conserved in mice, and the *NCYM* gene is co-amplified with *MYCN* in human primary neuroblastomas (6). MYCN directly targets *NCYM* for transcriptional activation whereas NCYM stabilizes MYCN protein, forming a positive auto-regulatory loop (6, 7). NCYM expression caused metastatic tumors in *MYCN*/*NCYM* double transgenic mice and inhibited apoptotic cell death (6). However these results do not rule out the possibility that NCYM is involved in other cellular phenotypes to promote the aggressiveness of neuroblastoma.

Neuroblastomas originate from neural crest cells that differentiate into multiple cell lineages (8). Some neuroblastoma cells retain multipotency and highly express stem cell-related genes, such as OCT4 (9) and LIN28 (10). Intermediate (I)-type neuroblastoma cells highly express OCT4 and differentiate into neuroblastic (N)-type or substrate adherent (S)-type cells in response to retinoic acid or BrdU treatment, respectively (11). $OCT4^{+}$/Tenascin C^{+} neuroblastoma cells were reported to serve as progenitors of tumor-derived endothelial cells, promoting neovascularization of the tumors (9). Furthermore, OCT4 is expressed in side-population cells of neuroblastoma (12). Despite these correlations between OCT4 expression and the stem cell-like state of neuroblastomas, the functional roles of OCT4 in neuroblastoma pathogenesis remain unclear. In this study, we investigated the biological and clinical significance of OCT4 in neuroblastomas and found that the newly evolved network between MYCN, NCYM and OCT4 regulates aggressiveness of human neuroblastomas.

Results

High expression of *OCT4* was associated with poor prognoses in *MYCN*-amplified human neuroblastomas

To examine the prognostic significance of *OCT4* mRNA expression in human neuroblastoma, total RNA was extracted from 36 *MYCN*-amplified and 67 *MYCN*-non-amplified primary neuroblastomas and subjected to quantitative real-time RT-PCR. Kaplan–Meier analysis showed that high levels of *OCT4* mRNA expression were significantly associated with poor outcomes in *MYCN*-amplified human neuroblastomas (Figure 1A), but not in *MYCN*-non-amplified human neuroblastomas (Figure 1B).

The expression levels of *OCT4* were correlated with prognostic factors

We next checked the relationship between the expression of *OCT4* and prognostic factors. The expression levels of *OCT4* were significantly correlated with International Neuroblastoma Staging System (INSS) stage, Shimada pathology and expression of *NCYM* and *MYCN* in *MYCN*-amplified primary neuroblastomas (Table 1). In addition, univariate Cox regression analysis of 36 *MYCN*-amplified primary neuroblastomas indicated that high levels of *OCT4* mRNA expression tended to correlate with poor

prognosis (Table S1). Multivariate Cox regression analysis also revealed that *OCT4* mRNA expression was not independent of *NCYM* and *MYCN* mRNA expression in *MYCN*-amplified primary neuroblastomas (Table S2).

NCYM induced *OCT4* via induction of MYCN

We next examined the factors that predict *OCT4* expression in primary neuroblastomas by multiple regression analysis (Table S3). The expression levels of *NCYM*, *NANOG*, *KLF4*, and c-*MYC* and *MYCN* amplification significantly contributed to the prediction of *OCT4* expression in primary neuroblastomas (Table S3). Furthermore, the expression levels of *NCYM* mRNA were positively correlated with those of *OCT4* and *NANOG*, whereas *KLF4* expression was inversely correlated with that of *MYCN* and *NCYM* (Table S4).

These results prompted us to assess whether NCYM regulates OCT4 as well as stem cell-related genes in human neuroblastoma cells. Overexpression of NCYM or MYCN, but not c-MYC, induced *OCT4* mRNA expression (Figure S1 and S2) as well as *NANOG*, *LIN28* and *SOX2*, whereas NCYM or MYCN did not enhance c-*MYC* or *KLF4* (Figure S1). Knockdown of NCYM decreased OCT4 and MYCN expression at both mRNA and

protein levels (Figure 2A and B), and suppressed their promoter activities (Figure 2C). A previous report suggested that MYCN is directly recruited onto the distal enhancer of human *OCT4* (14). We thus checked the recruitment of MYCN onto putative E-box sites found in human OCT4 enhancer regions (Figure 2D). Endogenous MYCN protein was recruited onto the distal enhancer region (Figure 2D and E, #1), but not in the proximal enhancer region (Figure 2D and E, #2). NCYM knockdown diminished MYCN binding to the distal enhancer of OCT4 (Figure 2E). Together these results suggest that NCYM regulates *OCT4* transcription via induction of MYCN.

In sharp contrast to human neuroblastoma cells, overexpression of NCYM in mice did not induce stem cell-related genes both *in vitro* (Figure S3) and *in vivo* (Figure S4). Furthermore, the E-box at the distal enhancer region of OCT4 is not evolutionally conserved among species (Figure S5A).

OCT4 directly stimulated *MYCN* transcription in human neuroblastoma

OCT4, SOX2 and NANOG form core networks in embryonic stem (ES) cells by their mutual transcriptional regulations (15). We thus examined whether OCT4 regulates *MYCN*/*NCYM* transcription in human neuroblastoma cells. In BE (2)-C

MYCN-amplified neuroblastoma cells, shRNA-mediated knockdown of OCT4 downregulated NCYM and MYCN at both the mRNA and protein levels (Figure 3A and B). Overexpression of OCT4 induced the expression and promoter activities of *MYCN* and *NCYM* in SK-N-AS *MYCN*-non-amplified neuroblastoma cells (Figure S6). In BE (2)-C cells, OCT4 knockdown suppressed the promoter activities of *OCT4* and *MYCN*, whereas it did not affect *NCYM* promoter activity (Figure 3C). These results suggest that OCT4 may not directly affect *NCYM* transcription at the endogenous expression levels. Overexpression of OCT4 enhanced activities of MYCN reporter constructs containing the intron 1 region of *MYCN* (Figure 3D). We found two putative OCT4 binding sites within the intron 1 region, and generated luciferase reporter constructs harboring mutations in the OCT4 binding sites (Figure 3E). Mutations in the upstream OCT4 binding sequence diminished OCT4-mediated enhancement of *MYCN* promoter activity, whereas *MYCN* promoter constructs containing the wild-type upstream OCT4 site sustained the response to OCT4 overexpression (Figure 3E). Chromatin immunoprecipitation (ChIP) assay showed that OCT4 was directly recruited onto the intron 1 region of MYCN (Figure 3F and G, #3). We also observed the recruitment of OCT4 to the promoter of MYCN (Figure 3F and G, #2), although the OCT4 site in the MYCN promoter was not responsible for OCT4-mediated enhancement of MYCN

promoter activity (Figure 3E). We next checked the conservation of the OCT4 binding site within intron 1 among species, and found that it is mostly conserved among primates, but not in mice (Figure S5B).

OCT4 is downregulated upon differentiation of neuroblastoma cells

BE (2)-C I-type neuroblastoma cells are stem cell-like cells that show the ability to differentiate into N-type cells in response to retinoic acid treatment (11) and MYCN expression is downregulated during the differentiation (11). We assessed the expression of NCYM and OCT4 in BE (2)-C I-type cells treated with ATRA (Figure 4A and B). As reported previously (11), BE (2)-C I-type cells differentiated into N-type cells with marked neurite extensions (Figure 4C and D), accompanied by a rapid decrease of MYCN expression (Figure 4A and B). The decrease of MYCN was followed by the downregulations of *NCYM*, *OCT4* and *SOX2* (Figure 4A and B), whereas no significant changes were observed in the expression levels of *NANOG* (Figure 4A). In good accordance with the strong correlation in primary tumors (Table S4), *NCYM* and *OCT4* expressions showed similar expression patterns in ATRA-treated BE (2)-C cells (Figure 4A and B). Furthermore, ATRA treatment decreased MYCN binding to the distal enhancer of *OCT4* (Figure 4E) and OCT4 binding to the intron 1 region of *MYCN*

(Figure 4F). Therefore, retinoic acid-induced neuronal differentiation abrogated the positive auto-regulatory loops formed by MYCN, NCYM and OCT4 via the simultaneous downregulation of their expressions.

OCT4 and NCYM maintain self-renewal of neuroblastoma cells

We next examined whether OCT4 and NCYM contributes to self-renewal of neuroblastoma cells. Knockdown of NCYM or OCT4 in BE (2)-C cells inhibited neurosphere formation (Figure 5B and C) and cellular invasion (Figure 5D and E), whereas the cell proliferations were not significantly changed within 3 days after shRNA transduction (Figure 5A). Izumi *et al.* recently reported that neuroblastoma cells have stem cell-like characteristics showing both asymmetric and symmetric cell divisions (SCD) *in vitro* and that MYCN suppresses the ACD (16). Consistent with the previous report (16), immunocytochemistry analyses showed a high percentage of cells exhibiting ACD in SK-N-AS *MYCN*-non-amplified cells compared with BE (2)-C *MYCN*-amplified cells (Figure S7). shRNA-mediated knockdown of NCYM or OCT4 significantly increased the number of cells exhibiting ACD in BE (2)-C cells (Figure 5F and G). Collectively, these results suggest that NCYM and OCT4 maintain self-renewal of human neuroblastoma cells.

Discussion

Here, we found that OCT4 promotes aggressiveness of *MYCN*-amplified neuroblastoma cells by forming a positive regulatory loop with MYCN/NCYM. Despite a correlation between OCT4 expression and a stem cell-like state of neuroblastomas, the clinical significance of OCT4 in neuroblastomas has remained elusive. In this study, we found that OCT4 was correlated with NCYM expression and undifferentiated pathological characteristics in Shimada pathology. Furthermore, the expression levels of OCT4 were associated with unfavorable outcomes in the *MYCN*-amplified tumors, but not in the *MYCN*-non-amplified tumors. A previous study showed that *MYCN* expression was inversely correlated with c-*MYC* in neuroblastoma (17). Moreover, low expression levels of *KLF4* mRNA were associated with poor neuroblastoma outcome (18). Our results showed that *NCYM* was also positively correlated with *NANOG* expression and was inversely correlated with *KLF4* and c-*MYC*. *In vitro* experiments showed that overexpression of NCYM induced *OCT4*, *SOX2* and *NANOG*, but not c-*MYC* or *KLF4*. Thus, among stem cell-related genes, NCYM mainly regulated the transcription of genes related to maintenance of pluripotency of ES cells (19-21) in human neuroblastoma cells. NCYM stabilized MYCN to stimulate *OCT4* transcription whereas OCT4 induced *NCYM* and *MYCN* via direct transcriptional activation of *MYCN*.

Therefore, MYCN, NCYM and OCT4 cooperate to induce each other, resulting in keeping their own expression at high levels and maintaining self-renewal of cells in *MYCN*-amplified neuroblastomas. Differentiation-inducing therapy by retinoic acid treatment has improved the overall survivals of *MYCN*-amplified neuroblastomas (22), and ATRA treatment abrogated the mutual transcriptional regulations between MYCN, NCYM and OCT4, inducing neuroblastoma cell differentiation. Previous studies have shown that OCT4 positive neuroblastoma cells have resistant potency to conventional therapy (12) and multipotency to differentiation (9). Therefore, the disruption of MYCN/NCYM-OCT4 network could be a good therapeutic strategy for aggressive tumors.

Previous reports have shown the physiological roles of OCT4 in the transcriptional regulation of *MYC* family members in various species (23). OCT4 stimulates *MYC* transcription for cell proliferation in human and mouse ES cells (24) and activates mych transcription for cell survival during zebrafish gastrulation (25). In the present study, we found the pathological significance of OCT4 for *MYCN* transcription in human neuroblastoma cells. The OCT4 binding sequence in *MYCN* intron 1 is not present in mice, but it is mostly conserved in other mammals. Although the E-box responsible for

MYCN-mediated *MYCN*/*NCYM* transcription is highly constrained in mammalians (Figure S8), NCYM coding sequences are conserved only in humans and monkeys (6). Therefore, the transcriptional regulation of *MYCN* by OCT4 and the positive auto-regulation of MYCN may have evolved before the emergence of the *NCYM* gene, and NCYM strengthens the MYCN-OCT4 network by stabilizing MYCN, thereby inducing *OCT4* transcription. *NCYM* is positively selected during evolution (6); however, its physiological roles in normal stem have remained unknown. Because new genes have been reported to rapidly become essential after emergence (26, 27), future studies will need to examine the physiological roles of the MYCN/NCYM-OCT4 networks in the maintenance of human normal stem cells.

Materials and Methods

Clinical specimens

Tumor RNA samples were obtained from 36 *MYCN*-amplified and 67 *MYCN*-non-amplified tumor specimens in our Neuroblastoma Resource Bank at the Chiba Cancer Center Research Institute. The specimens were kindly provided from various institutions and hospitals where informed consent was obtained. All tumors were diagnosed clinically as well as pathologically as neuroblastoma and staged according to the INSS criteria. Total RNA was extracted from each frozen tissue according to the previous report (13).

Cell culture

The human neuroblastoma cell line SK-N-AS (*MYCN*-non-amplified) was maintained in RPMI 1640 medium (Wako, Osaka, Japan) supplemented with 10% heat-inactivated fetal bovine serum (FBS) (Gibco, Life Technologies, Carlsbad, CA, USA). The other human neuroblastoma cell line BE (2)-C (*MYCN*-amplified) was cultured in a 1:1 mixture of minimal essential medium (Gibco) and Ham's Nutrient Mixture F-12 (Gibco) supplemented with 15% heat-inactivated FBS (Gibco) with 1% MEM nonessential amino acids (Gibco). Mouse neuroblastoma Neuro2a cells and HEK293T cells were cultivated in Dulbecco's modified Eagle's medium (Wako) supplemented with 10% heat-inactivated FBS (Gibco).

Overexpression of NCYM, OCT4, and MYCN in neuroblastoma cell lines

We previously constructed a pcDNA3-FLAG-NCYM that expresses NCYM fused to the FLAG epitope at the NH2 terminus and cloned into the pcDNA3.1. (pcDNA3) vector (Promega, Southampton, UK) and pcDNA3-MYCN (6). The OCT4 complementary DNA was digested from pCR-TOPO-OCT4 (Funakoshi, Tokyo, Japan) by EcoRI and introduced into a pcDNA3 expression vector. The sequence of the entire OCT4 open reading frame was confirmed by sequencing. Before transient transfection, cells were seeded at 1×10^5 cells/mL in a dish and allowed to adhere overnight. Transient transfection was performed using Lipofectamine 2000 transfection reagent (Invitrogen, Karlsruhe, Germany) according to the manufacturer's instructions. Cells were analyzed 48 hours after the transfection.

Gene knockdown assay

The following gene-specific shRNAs were used: NCYM sh-1 (N-cym 1 custom shRNA; Sigma, St Louis, MO, USA) 5′-tggcaattgcttgtcattaaa-3′, NCYM sh-2 (N-cym 2 custom shRNA; Sigma) 5′-gaggttgctcctgtgtaatta-3′, OCT4 sh-1 (TRCN0000004879; Sigma) 5′-ccggtcattcactaaggaaggaattctcgagaattccttccttagtgaatgattttt-3′, OCT4 sh-2 (TRCN0000004881, Sigma) 5′-ccggccctcacttcactgcactgtactcgagtacagtgcagtgaagtgagggttttt-3′ and control shRNA (Non-Target shRNA SHC002) were purchased from Sigma. The lentivirus was produced by

co-transfecting pCMVR and pMDG plasmids into HEK293T cells. Before the co-transfection, cells were seeded at 2×10^5 cells/mL in a dish and allowed to adhere overnight. Co-transfection was performed using FuGENE HD reagent (Roche, Mannheim, Germany) according to the manufacturer's instructions. At 24 and 48 hours after transfection, the viral supernatants were collected and mixed with culture medium. Neuroblastoma cells were cultured for 12 hours in a 1:1 mixture of viral supernatants and culture medium. All shRNA-mediated knockdown cells were subjected to experiments 72 hours after infection.

All-*trans* retinoic acid (ATRA) treatment

ATRA was purchased from Wako and diluted to 5 mM for experimental use. ATRA was added at the final concentration of 5 μM 24 hours after cell seeding at 2×10^5 cells/mL for each experiment.

Quantitative real-time RT-PCR analysis

Total RNA was isolated from the frozen tumor samples of transgenic mice with Isogen (Nippon Gene, Tokyo, Japan), and treated with RNase-free DNase I. Total RNA was prepared from primary neuroblastoma tissues and cell lines, followed by first-strand synthesis. Quantitative real-time RT-PCR was carried out using the SYBR Green and Taqman method as described by the manufacturer (Applied Biosystems, Foster City, CA, USA). Primer sets used are as follows: *NCYM*

(endogenous) 5′-CTAGAGCCGAGGGAATTTCTTTT-3′ and 5′-CCCAGCTTTGCAGCCTTCT-3′, *NCYM* 5′-CGCCCCCTTAGGAACAAGAC-3′ and 5′-GCGCCCCTCTTCTTTCAATT-3′, *MYCN* (endogenous) 5′-TCCATGACAGCGCTAAACGTT-3′ and 5′-GGAACACACAAGGTGACTTCAACA-3′, *MYCN* 5′-CCTTCGGTCCAGCTTTCTCA-3′ and 5′-GGCCTTCTCATTCTTTACCAACTC-3′, *OCT4* (endogenous) 5′-GGGTTTTTGGGATTAAGTTCTTCA-3′ and 5′-GCCCCCACCCTTTGTGTT-3′, *OCT4* 5′-CGACCATCTGCCGCTTTG-3′ and 5′-GCCGCAGCTTACACATGTTCT-3′, *NANOG* 5′-CCAAAGGCAAACAACCCACTT-3′ and 5′-CGGGACCTTGTCTTCCTTTTT-3′, *SOX2* 5′-ACAGCAAATGACAGCTGCAAA-3′ and 5′-TCGGCATCGCGGTTTTT-3′, *KLF4* 5′-ACCAGGCACTACCGTAAACACA-3′ and 5′-ATGCTCGGTCGCATTTTTG-3′, c-*MYC* 5′-AGGGTCAAGTTGGACAGTGTCA-3′ and 5′-TGGTGCATTTTCGGTTGTTG-3′. The mRNA levels of genes were standardized by *β-actin* or *GAPDH*.

Western blotting

We resolved cell proteins by SDS-PAGE prior to electroblotting onto a PVDF membrane. We incubated the membranes with the following primary antibodies overnight: anti-NCYM (1:1000 dilution; (6)), anti-OCT4 (1:1000 dilution; Cell Signaling Technology, Danvers, MA, USA), anti-MYCN (1:1000 dilution; Calbiochem, San Diego, CA, USA), and anti-actin (1:2000 dilution;

Sigma). The membranes were then incubated with a horseradish peroxidase-conjugated secondary antibody (anti-rabbit IgG at 1:2000 dilution or anti-mouse IgG at 1:2000 dilution; Cell Signaling Technology) and the bound proteins were visualized using a chemiluminescence-based detection kit (ECL and ECL pro kit; Amersham, Piscataway, NJ, USA).

Chromatin immunoprecipitation (ChIP) assay

BE (2)-C cells were infected with lentivirus of shNCYM, shOCT4, or shMYCN. ChIP assays were performed with a ChIP assay kit (Millipore, Temecula, CA, USA) according to the manufacturer's instructions using anti-NCYM (6), anti-OCT4 (Cell Signaling Technology), anti-MYCN (Calbiochem), normal mouse IgG (Jackson ImmunoResearch Laboratories Inc., Suffolk, UK), or normal rabbit IgG (Jackson ImmunoResearch Laboratories Inc.). The primer sequences for the OCT4 and MYCN promoters were as follows: OCT4 promoter 1 5′-GAGGATGGCAAGCTGAGAAA-3′ and 5′-CTCAATCCCCAGGACAGAAC-3′, OCT4 promoter 2 5′-GTTGGGGAGCAGGAAGCA-3′ and 5′-GGGGCAGCTCTAACCCTAAA-3′, MYCN promoter 1 5′-GACAGCACTTCCATCTCGGTAAA-3′ and 5′-GCCACCATTCTCCCCAGTT-3′, MYCN promoter 2 5′-GGCGCCTCCCCTGATTT-3′ and 5′-GAGGGAGAAAGGAGAGGAAAGC-3′, MYCN promoter 3 5′-CTGTCGTAGACAGATTGTAC-3′ and 5′-AACCAGGTTCCCCAATCTTC-3′

Luciferase reporter assay

MYCN (−221/+1312), MYCN (−1030/+21), and NCYM-luc (−149/+1384) plasmids (where +1 represents the transcription start site) were generated in previous reports (6, 7). We then subcloned the *MYCN* promoter region (−221/+465) into the pGL3-basic vector using MYCN (−221/+1312) as a template. *MYCN* promoter (−221/+409) and *MYCN* promoter (−221/+210) were made by PCR-based amplification using *MYCN* promoter (−221/+465) as a template. Putative OCT4 binding site wild-type and mutant of *MYCN* promoter were generated from *MYCN* promoter (−221/+465). Primer sets used were as follows: 5′-GCAGCCTTCTCTCTGCAAAG-3′ (forward) and 5′-CCTAATCCTTTTGCAGCCC-3′ (reverse, *MYCN* promoter −221/+409 putative OCT4 binding site WT), 5′-CCTAATCCTTTTACAGCCC-3′ (reverse, *MYCN* promoter −221/+409 putative OCT4 binding site MT1), 5′-CCTAATCCTTTTACTGCCC-3′ (reverse, *MYCN* promoter −221/+409 putative OCT4 binding site MT2), 5′-GCAGGGCTTGCAAACCGCCC-3′ (reverse, *MYCN* promoter −221/+201 putative OCT4 binding site WT) or 5′-GCAGGGCTTGGAAAGCGCCC-3′ (reverse, *MYCN* promoter −221/+201 putative OCT4 binding site MT). Underlined sequences in the reverse primers indicate the wild-type or mutated OCT4 binding site. *OCT4* promoter sequences containing the *OCT4* promoter regions at nucleotides −4991 to +77 from the transcription start site were obtained from Addgene (Cambridge, MA, USA). shRNA-transfected BE (2)-C, SK-N-AS and

Neuro2a cells were seeded at 5×10^4 cells/well in a 12-well plate and allowed to adhere overnight. SK-N-AS and Neuro2a cells were co-transfected the following day with empty vector (pcDNA3), pcDNA3-FLAG-NCYM, pcDNA3-OCT4, or pcDNA3-MYCN along with 400 ng of NCYM, OCT4, or MYCN luciferase reporter construct and 40 ng of *Renilla* TK with Lipofectamine 2000 (Invitrogen). At 48 hours after the second transfection, the cells were harvested and the luciferase activity was determined using a dual luciferase assay system (Promega) according to the manufacturer's instructions.

Migration and invasion assay

The invasive potential of neuroblastoma cells *in vitro* was evaluated using Matrigel-coated Transwell inserts (BD Biosciences, San Jose, CA, USA) according to the manufacturer's instructions. BE (2)-C cells transfected with the control shRNA or NCYM sh-1 and OCT4 sh-1 were seeded onto an insert with 8-μm pores (BD Biosciences) in a 24-well plate at 1×10^5 cells/mL. After 48 hours, cells on the lower side of the membrane were fixed with 4% paraformaldehyde and stained using a Diff Quick Staining Kit (Sysmex, Kobe, Japan). Stained cells were counted. Invading cells were standardized by migrating cells.

Cell proliferation assay

shRNA-transfected neuroblastoma cells were seeded in 96-well plates at a density of 5×10^3 cells per well in a final volume of 100 μL. The absorbance of each well was measured using a Dynatech MR5000 plate reader with a test wavelength of 450 nm and a reference wavelength of 630 nm. WST assay was performed according to the manufacturer's instructions (Cell Counting Kit-8; Dojindo, Kumamoto, Japan).

Sphere formation assay

We evaluated neurospheres derived from BE (2)-C cells transfected with the indicated shRNA. We plated cells at 5×10^4 cells/mL in 60-mm dishes to check the sphere morphology, and used a 96-well plate to count the spheres. The cells were allowed to proliferate in serum-free DMEM (Sigma) and F12 medium (Invitrogen) containing epidermal growth factor (Sigma) and 20 ng/mL basic fibroblast growth factor (Invitrogen) with 2% B27 supplement (Invitrogen). After 72 hours, colonies with diameters >100 μm were counted.

Immunofluorescence analysis

BE (2)-C and SK-N-AS cells were grown on coverslips and transfected with indicated shRNAs. Cells were fixed in 4% paraformaldehyde for 15 min at room temperature, blocked in 3% bovine serum albumin, stained with the indicated antibodies, and examined with a laser scanning confocal

microscope (DMI 4000B; Leica, Wetzlar, Germany).

Asymmetric cell division (ACD) assay

We tested whether neuroblastoma cells showed asymmetric distribution of NuMA. Asymmetric distributions of NuMA to one side of the cell were counted during mitotic stages. The spindle apparatus were also stained with anti-tubulin-α antibody to avoid false results caused by uneven dyeing. The antibodies used were as follows: anti-NuMA (Novus Biologicals, Littleton, CO, USA), and anti-tubulin-α (Thermo Fisher Scientific, Wilmington, DE, USA).

Statistical analysis

All data were presented as the mean ± standard deviation and were obtained from three independent experiments. Statistical significances in the clinical data were calculated using the log-rank test, Chi-square test, and Student's *t*-test. Hazard ratios were calculated using univariate and multivariate Cox regression analysis. Statistical analyses were performed with JMP® 9 (SAS Institute Japan, Tokyo, Japan). Statistical significance was set at $P < 0.05$.

Figure & Table

Fig. 1 Kaneko *et al.*,

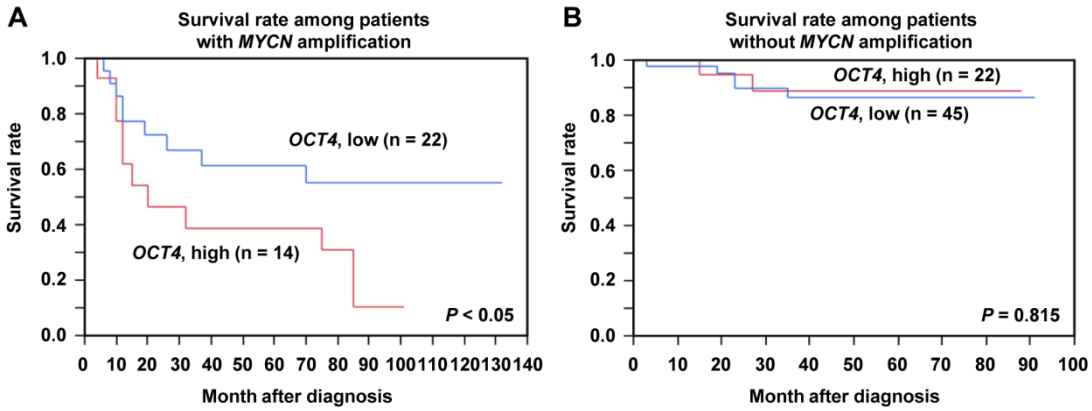

Table 1. Prognostic significance of *OCT4* expression and other clinical factors in *MYCN*-amplified neuroblastomas (Chi-square test).

Factor		*OCT4* expression		*P*-value
		Low (n = 22)	High (n = 14)	
Age (month)	<18 (n = 22)	11	11	0.079
	≧18 (n = 14)	11	3	
INSS stage (3 or 4)	3 (n = 9)	8	1	<0.05
	4 (n = 27)	14	13	
Tumor origin	Adrenal gland (n = 32)	19	13	0.534
	Others (n = 4)	3	1	
Shimada classification	Favorable (n = 6)	6	0	<0.001
	Unfavorable (n = 30)	16	14	
MYCN expression	Low (n = 25)	18	7	<0.05
	High (n = 11)	4	7	
NCYM expression	Low (n = 26)	21	5	<0.001
	High (n = 10)	1	9	

Fig. 2 Kaneko *et al.*,

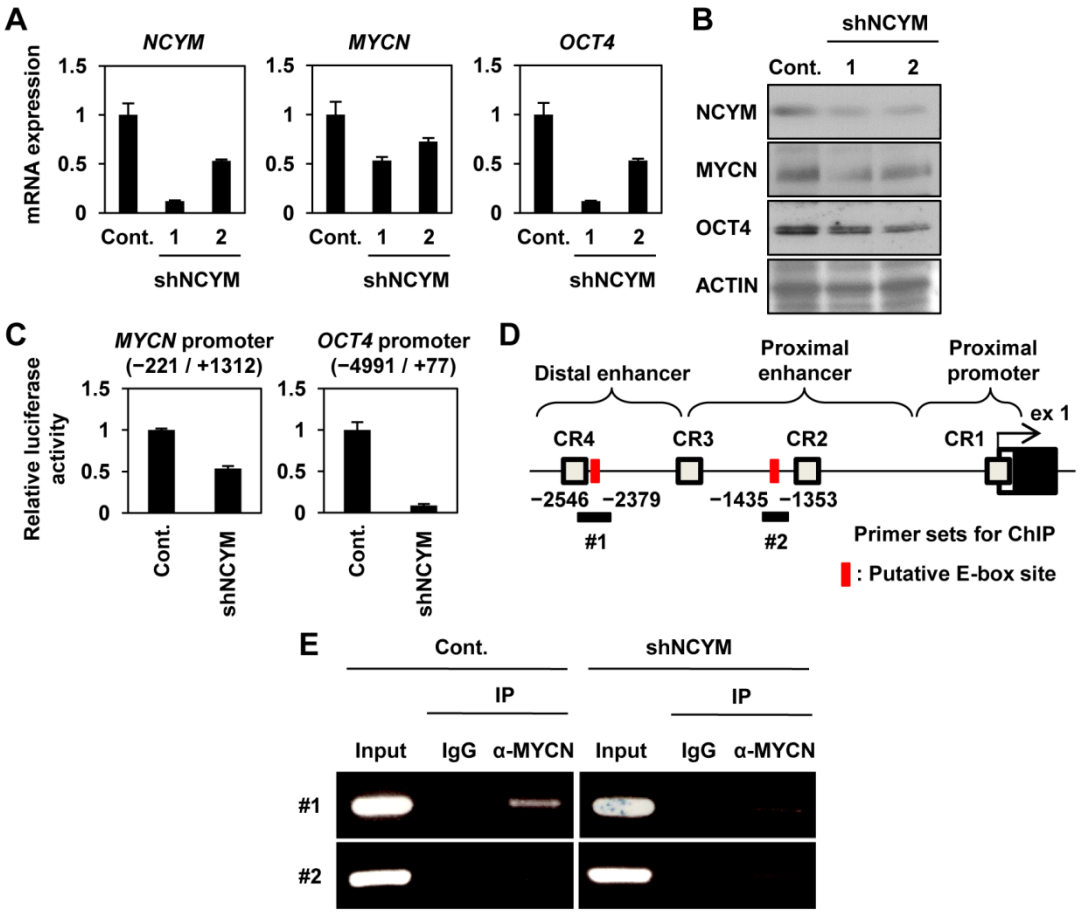

Fig. 3

Kaneko *et al.*,

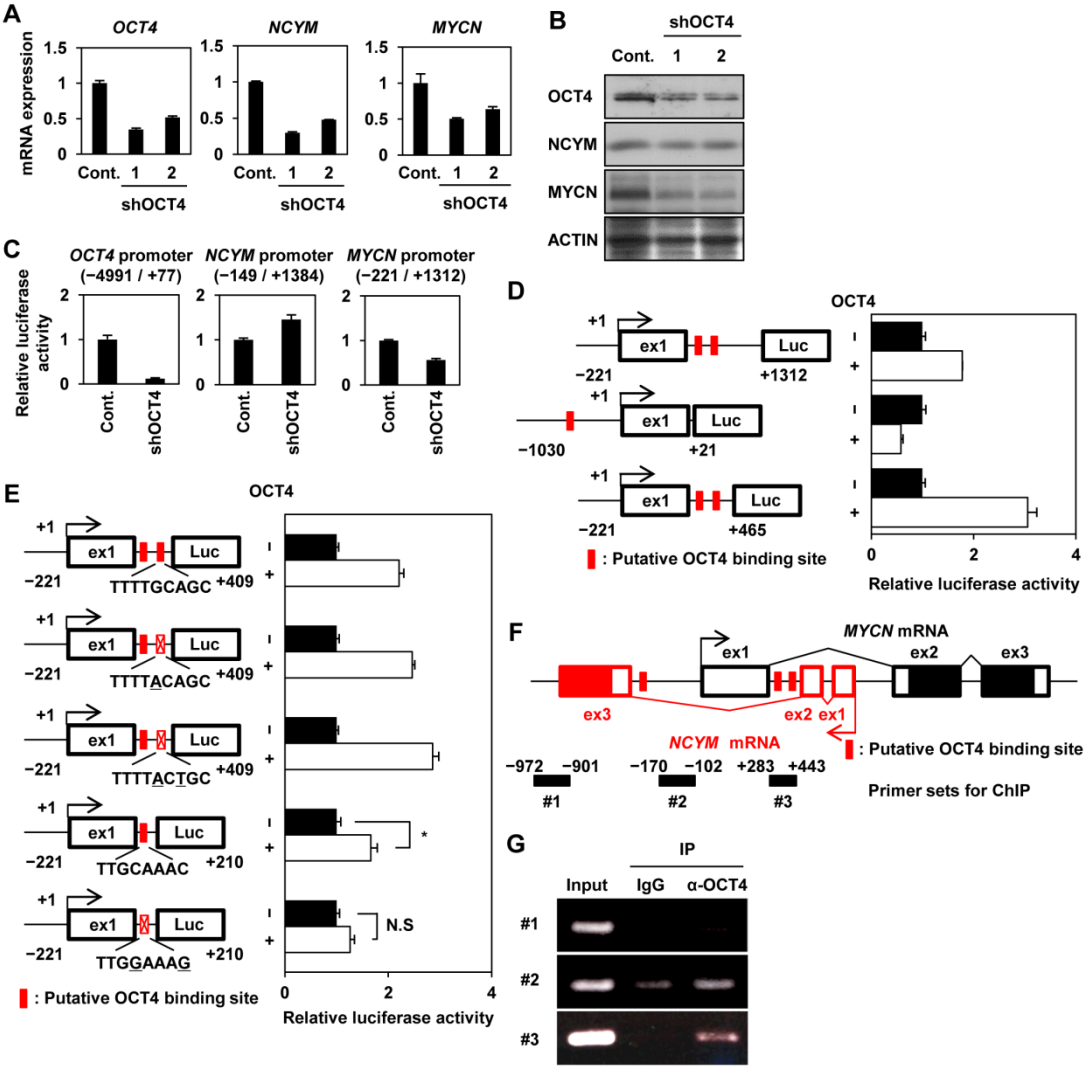

Fig. 4 Kaneko *et al.*,

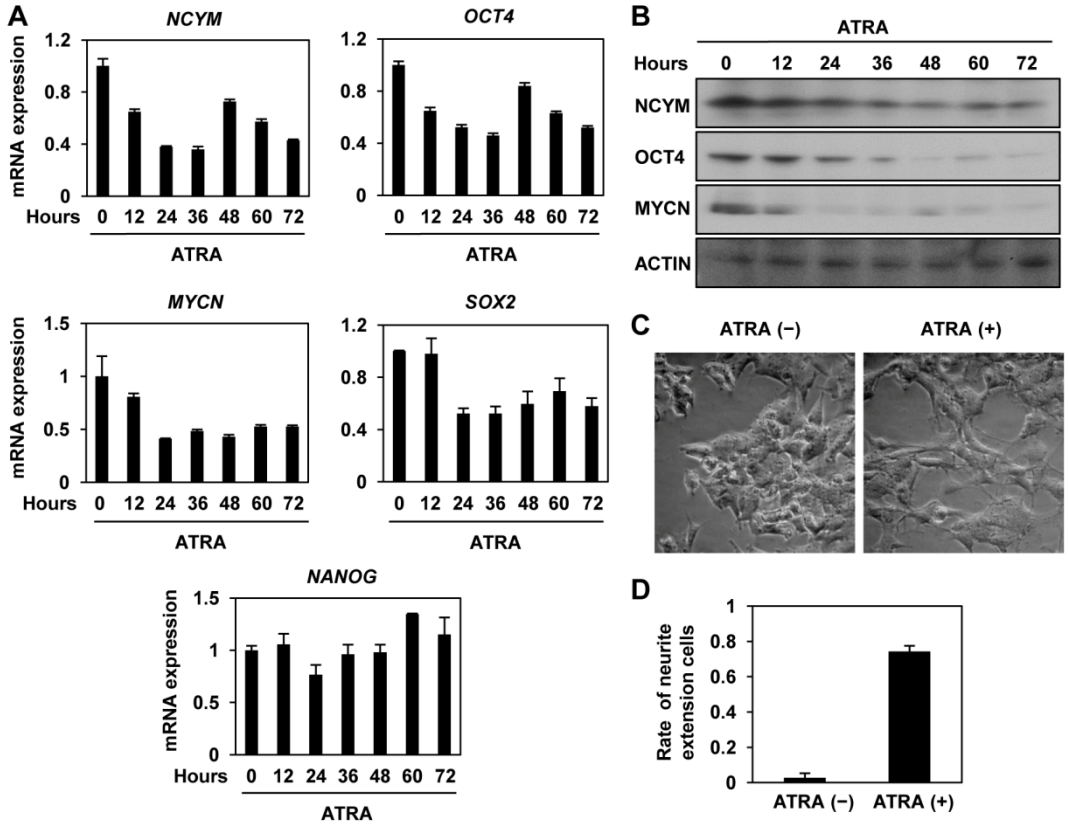

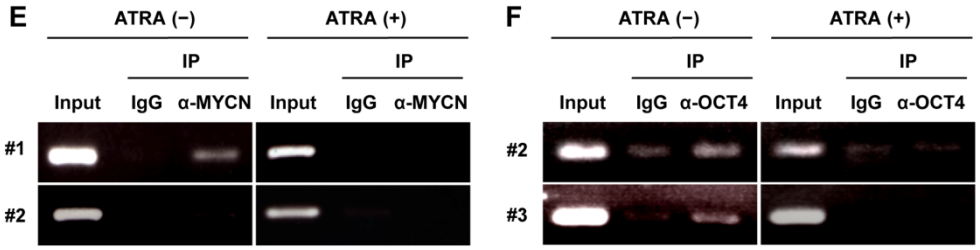

Fig. 5

Kaneko *et al.*,

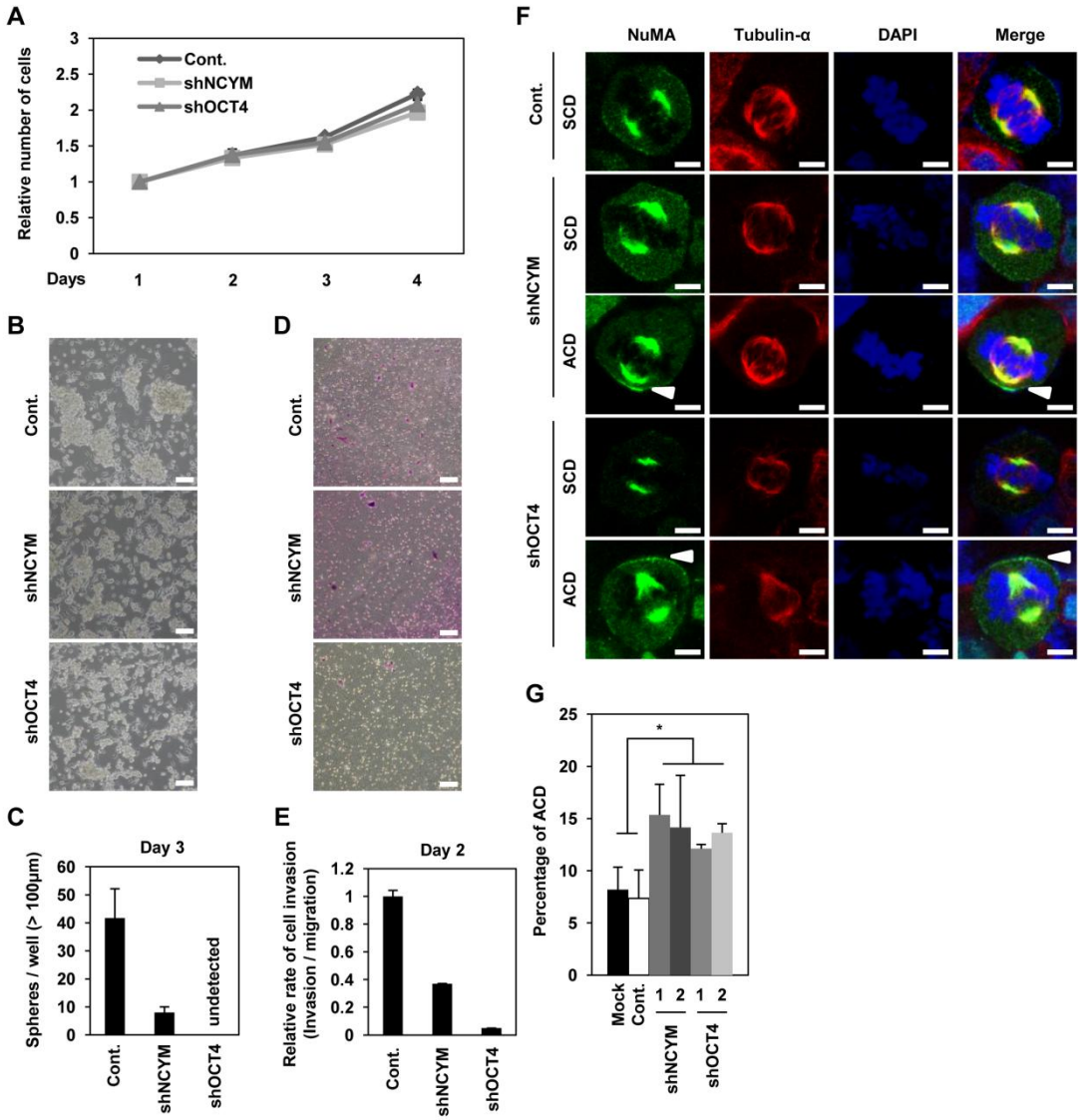

Figure Legends

Figure 1. High *OCT4* expression correlates with unfavorable prognosis in human *MYCN*-amplified neuroblastomas. (A) Overall survival of *MYCN*-amplified neuroblastomas according to relative *OCT4* expression levels (n = 36; high, n = 14; low, n = 22). *P*-value by log-rank test. (B) Overall survival of *MYCN*-non-amplified neuroblastomas according to relative OCT4 expression levels (n = 67; high, n = 22; low, n = 45). *P*-value by log-rank test.

Table 1. Prognostic significance of *OCT4* expression and other clinical factors in *MYCN*-amplified neuroblastomas (Chi-square test).

Figure 2. NCYM regulates OCT4 via the recruitment of MYCN onto *OCT4* promoter region in neuroblastoma cells. (A) Quantitative real-time RT-PCR analyses of *NCYM*, *MYCN* and *OCT4* in NCYM shRNA-transfected BE (2)-C neuroblastoma cells. Three days after infection, mRNA expression levels were measured by real-time RT-PCR with *β-actin* as an internal control. (B) Western blot analyses of NCYM, MYCN, and OCT4 proteins in NCYM shRNA-transfected BE (2)-C neuroblastoma cells. Three days after infection, cells were subjected to western blot analyses. ACTIN was used as loading control. (C) Luciferase activity of *MYCN* and *OCT4* reporters in NCYM shRNA-transfected BE (2)-C neuroblastoma cells. Seventy-two hours after infection, cells were

subjected to luciferase reporter assay. Data are shown as the fold change in the luciferase activity. The activities were standardized by control cells. (D) Schematic depiction of the *OCT4* promoter region. The *OCT4* promoter is divided into three regions (distal enhancer, distal promoter, and proximal promoter). Each conserved region (CR1-4) and translated region is boxed. The gray, white, and black boxes indicate the conserved region, non-coding region, and coding region, respectively. The locations of the chromatin immunoprecipitation (ChIP) primers are indicated by the bold lines. The putative E-box sites are shown in red boxes. (E) Identification of the MYCN binding region in the *OCT4* promoter by ChIP assays. BE (2)-C neuroblastoma cells were transfected with or without shRNA. Three days after infection, cells were subjected to ChIP assay. Genomic DNA was amplified by PCR by specific primer sets as shown by bold black lines #1 and #2 in panel D. PCR bands indicated in panel #1 indicated amplification of the distal enhancer region; PCR bands indicated in panel #2 indicate amplification of the proximal enhancer region.

Figure 3. OCT4 induced transcription of MYCN in neuroblastoma cells. (A) Quantitative real-time RT-PCR analysis of *NCYM*, *MYCN* and *OCT4* in OCT4 shRNA-transfected BE (2)-C neuroblastoma cells. Seventy-two hours after infection, mRNA expression levels were measured by real-time RT-PCR with *β-actin* as an internal control. (B) Western blot analyses of NCYM, MYCN and OCT4 proteins in OCT4 shRNA-transfected BE (2)-C neuroblastoma cells. Three days after infection, cells

were subjected to western blot analyses. ACTIN was used as loading control. (C) Luciferase activity of *OCT4*, *NCYM* and *MYCN* reporters after OCT4 shRNA-transfected BE (2)-C neuroblastoma cells. Seventy-two hours after infection, cells were subjected to luciferase reporter assay. Data are shown as the fold change in the luciferase activity. The activities were standardized by control cells. (D) Luciferase activity of *MYCN* (−221/+1312, −1030/+21 and −221/+465) reporters after OCT4 transfection of SK-N-AS neuroblastoma cells. Forty-eight hours after transfection, cells were subjected to luciferase reporter assay. Data are shown as the fold change in the luciferase activity. The activities were standardized by control cells. (E) Luciferase activity of *MYCN* reporters (−221/+409, −221/+409 mutant 1, −221/+409 mutant 2, −221/+210 mutant and −221/+409 mutant) after OCT4 transfection of SK-N-AS neuroblastoma cells. Two days after transfection, cells were subjected to luciferase reporter assay. Data are shown as the fold change in the luciferase activity. The activities were standardized by control cells. The putative OCT4 binding sites are indicated in red boxes. Statistical significance determined by the Student's *t*-test, $*P < 0.05$. (F) Schematic of the *MYCN*/*NCYM* promoter and coding region. These are divided into three exons (exon 1–3). Each translated region is boxed. The red and black boxes indicate the NCYM and MYCN regions, respectively. The locations of the chromatin immunoprecipitation (ChIP) primers are indicated by the bold line. The putative OCT4 binding sites are indicated by red boxes. (G) Identification of the OCT4 binding region in the *MYCN*/*NCYM* region by ChIP assays in BE (2)-C neuroblastoma cells.

Three days after infection, cells were subjected to ChIP assay. Genomic DNA was amplified by PCR using the primer sets shown in panel F.

Figure 4. All-*trans* retinoic acid-induced neuronal differentiation abrogated the positive auto-regulatory loops formed by OCT4, MYCN, and NCYM. (A) Quantitative real-time RT-PCR analysis of *NCYM*, *MYCN* and ES cell-related genes in ATRA-treated BE (2)-C neuroblastoma cells. mRNA expression levels were measured by real-time RT-PCR with *β-actin* as an internal control. (B) Western blot analyses of NCYM, MYCN and OCT4 proteins in ATRA-treated BE (2)-C neuroblastoma cells. ACTIN was used as loading control. (C) Morphology of BE (2)-C neuroblastoma cells treated with or without ATRA. (D) Percentage of BE (2)-C neuroblastoma cells with marked neurite extensions relative to control with or without ATRA treatment. Error bars represent SEM from three independent experiments. (E) Identification of the MYCN-binding region in the *OCT4* promoter by ChIP assays. BE (2)-C neuroblastoma cells were treated with or without ATRA. Genomic DNA was amplified by PCR using the primer sets shown in Figure 2D. (F) Identification of the OCT4 binding region in the *MYCN*/*NCYM* promoter by ChIP assays. BE (2)-C neuroblastoma cells were treated with or without ATRA. Genomic DNA was amplified by PCR using the primer sets shown in Figure 3F.

Figure 5. NCYM and OCT4 control cancer stem cell-like properties in neuroblastoma cells. (A) Cell viability assay of BE (2)-C neuroblastoma cells with NCYM or OCT4 shRNA-mediated knockdown. Cell proliferation was examined by WST assays at the indicated time points. (B) Sphere formation assay of BE (2)-C neuroblastoma cells. Representative images showing induction of sphere-forming activity after knockdown of NCYM and OCT4. Scale bars, 100 μm. (C) Quantification of sphere numbers from panel B. The numbers of spheres were counted 72 hours after infection. Error bars represent SEM from three independent experiments. (D) Invasion assay of BE (2)-C neuroblastoma cells. Representative images of showing invasion activity after knockdown of NCYM and OCT4. Scale bars, 100 μm. (E) Quantification of BE (2)-C neuroblastoma cells invading the Matrigel relative to control migration after NCYM and OCT4 shRNA-mediated knockdown from panel D. The numbers of spheres were counted 48 hours after infection. Error bars represent SEM from three independent experiments. (F) Representative images of symmetric distribution of NuMA during the late stage of mitosis in shRNA-treated neuroblastoma cells. Tubulin-α is indicated in red, NuMA is green and DNA is blue. Arrows show the distribution of NuMA on the cell cortex. Scale bars, 5 μm. (G) Quantification of cells with ACD in shRNA-transfected human neuroblastoma cells during late metaphase and anaphase. Error bars represent SEM from three experiments. Statistical significance determined by the Student's *t*-test, $*P < 0.05$.

Supporting Information

Fig. S1

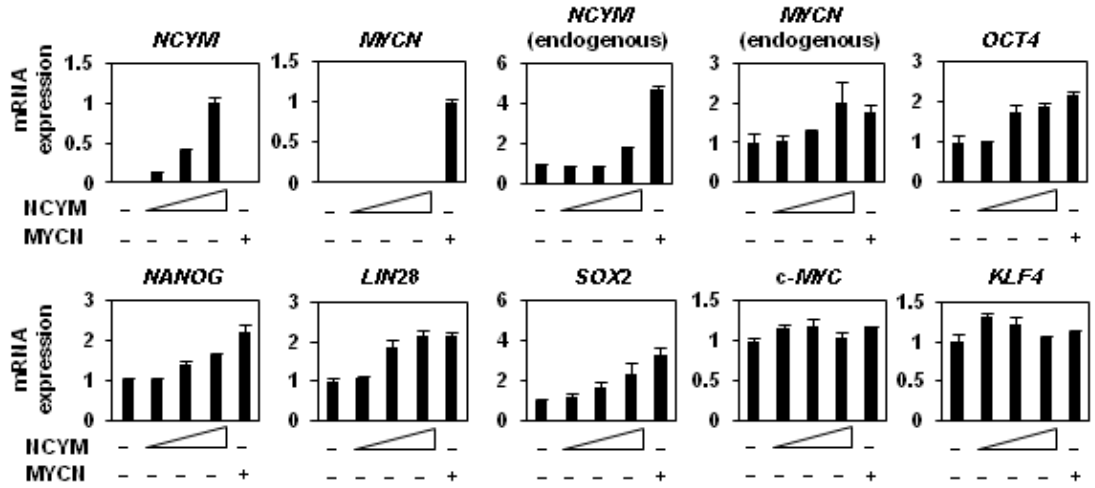

Fig. S2

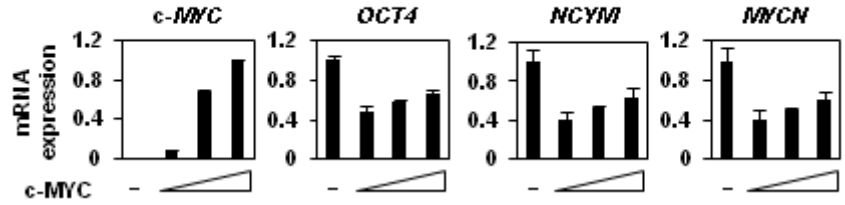

Fig. S3

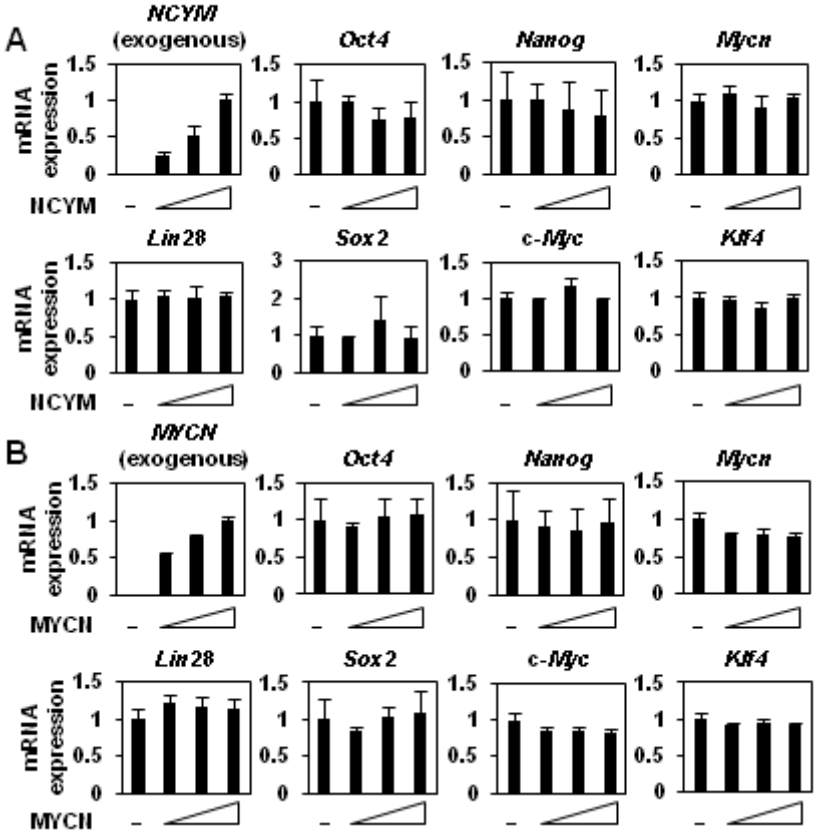
A
NCYM (exogenous)
Oct4
Nanog
Mycn
Lin28
Sox2
c-Myc
Klf4
mRNA expression
NCYM
B
MYCN (exogenous)
Oct4
Nanog
Mycn
Lin28
Sox2
c-Myc
Klf4
mRNA expression
MYCN

Fig. S4

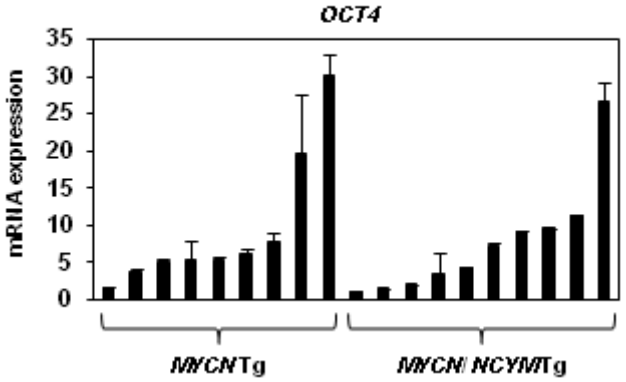

Fig. S5


A
OCT4 promoter
Human GAGAAGTGAAC---ACAGCTGCAACCCCA
Chimp GAGAAGTGAAC---ACAGCTCCAACCCCA
Gibbon GAGAAGTGAAC---ACCGCTCCAACACCA
Rhesus GAGAAGTGAAC---ACAGCTCCAACCGCA
Marmoset GAGAAGTGAAC---ACAGCTCCAGCTCCA
Horse CAGAGGTGAGT---ATAGCTCCAGCCCCA
Cat TAGAGGTGAAT---ACAGTTCCGGCACCA
Rabbit GCAG-GTGGGC---ACAGCTCCAGCGGCA
Sheep TAGAGGCAAAT---ATAGCTCCAATTTCG
Mouse -CTTTGTGAACTTGGCGGCTTCCAAGTCG
Rat GCCTTGGGAACTGGGTGGCTCCAGCTTCA
Chicken ==========
X. tropicalis ==========
Zebrafish ----------
B
MYCN/NCYM region
Human AGCAGGGCTTGCAAAC-CGCCCGGCG
Chimp AGCAGGGCTTGCAAAC-CGCCCGGCG
Gibbon AGCAGGGCTTGCAAAC-CGCCCGGCG
Rhesus AGCAGGGCTTCCAAAC-CGCCCGGCG
Marmoset AGCAGGGCTTGCAAAC-CGCCCGGCT
Horse AGCTTGGGTTGCAAAC-CGCCCGGCG
Cat AGCTGGGGTTGCAAAC-TGCCCGGCG
Rabbit AGCGGGGCTTTGCAAC-CGCCCGGCG
Sheep A----------CCGGCG
Mouse AGCGGTACTTGCGAGG-CTTCGAGCG
Rat AGCGGTACTTGCAAAC-CTCCGAGCG
Chicken ==========
X. tropicalis AGCGGAGCCTACTGACTGGGCTGGAA
Zebrafish ----------

Fig. S6

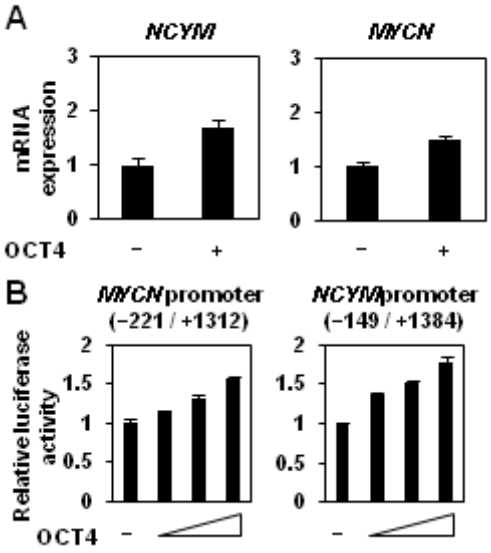
A
NCYM
MYCN
mRNA expression
3
2
1
0
OCT4
–
+
B
MYCN promoter
(−221 / +1312)
NCYM promoter
(−149 / +1384)
Relative luciferase activity
2
1.5
1
0.5
0
OCT4
–

Fig. S7

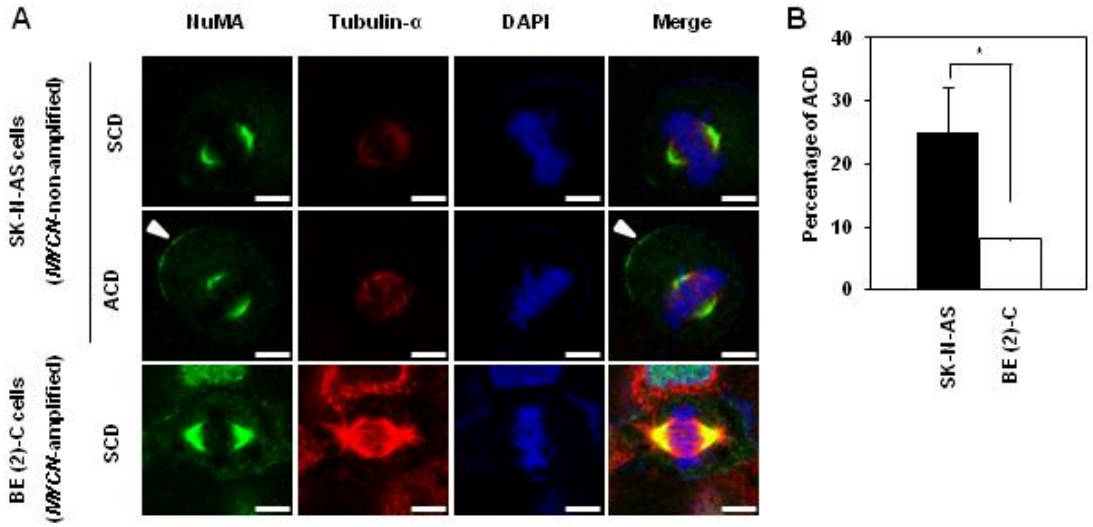
A
NuMA
Tubulin-α
DAPI
Merge
SK-N-AS cells (MYCN-non-amplified)
SCD
ACD
BE (2)-C cells (MYCN-amplified)
SCD
B
Percentage of ACD
40
30
20
10
0
*
SK-N-AS
BE (2)-C

Fig. S8

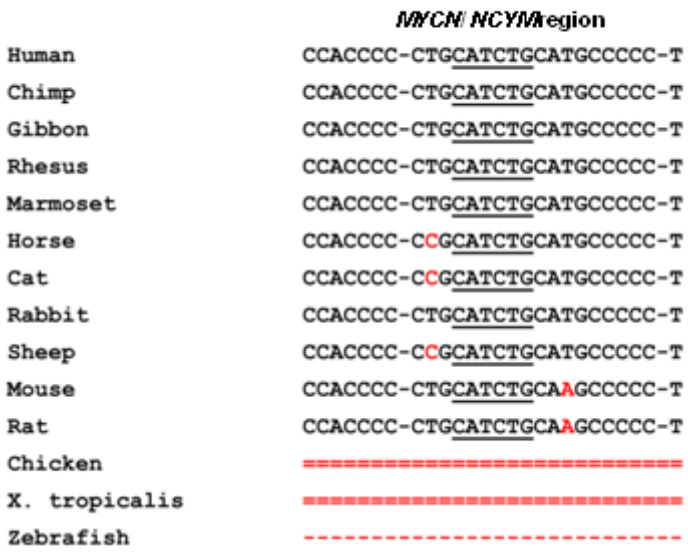
MYCN/*NCYM* region
Human CCACCCC-CTGCATCTGCATGCCCCC-T
Chimp CCACCCC-CTGCATCTGCATGCCCCC-T
Gibbon CCACCCC-CTGCATCTGCATGCCCCC-T
Rhesus CCACCCC-CTGCATCTGCATGCCCCC-T
Marmoset CCACCCC-CTGCATCTGCATGCCCCC-T
Horse CCACCCC-CCGCATCTGCATGCCCCC-T
Cat CCACCCC-CCGCATCTGCATGCCCCC-T
Rabbit CCACCCC-CTGCATCTGCATGCCCCC-T
Sheep CCACCCC-CCGCATCTGCATGCCCCC-T
Mouse CCACCCC-CTGCATCTGCAAGCCCCC-T
Rat CCACCCC-CTGCATCTGCAAGCCCCC-T
Chicken ==========
X. tropicalis ==========
Zebrafish ----------

Table S1. Univariate Cox regression analysis using *OCT4* expression level and clinical prognosis factors in *MYCN*-amplified neuroblastomas.

Factor	*P*-value	HR (95% CI)
Age (<18 vs. ≧18)	0.275	0.606 (0.249-1.512)
INSS stage (4 vs. 3)	0.445	1.508 (0.551-5.277)
Tumor origin (Adrenal gland vs. Others)	0.85	0.864 (0.241-5.507)
Shimada classification (Unfavorable vs. Favorable)	0.775	1.191 (0.398-5.113)
OCT4 expression (High vs. Low)	0.057	2.35 (0.971-5.838)
MYCN expression (High vs. Low)	0.516	1.351 (0.527-3.279)
NCYM expression (High vs. Low)	0.121	2.086 (0.813-5.074)

Table S2. Multivariate Cox regression analysis using *OCT4* expression level and clinical prognosis factors in *MYCN*-amplified neuroblastomas.

Model	Factor	*P*-value	HR (95% CI)
A	*OCT4* expression (High vs. Low)	<0.05	3.498 (1.307-9.837)
	Age (<18 vs. ≧18)	0.051	0.363 (0.13-1.005)
B	*OCT4* expression (High vs. Low)	0.082	2.385 (0.896-6.919)
	INSS stage (4 vs. 3)	0.952	0.962 (0.285-3.746)
C	*OCT4* expression (High vs. Low)	<0.05	2.476 (1.002-6.338)
	Tumor origin (Adrenal gland vs. Others)	0.582	0.637 (0.166-4.174)
D	*OCT4* expression (High vs. Low)	0.053	2.595 (0.986-7.542)
	Shimada classification (Unfavorable vs. Favorable)	0.645	1.394 (0.293-5.302)
E	*OCT4* expression (High vs. Low)	0.072	2.466 (0.919-6.711)
	MYCN expression (High vs. Low)	0.829	0.894 (0.314-2.427)
F	*OCT4* expression (High vs. Low)	0.256	2.083 (0.565-6.694)
	NCYM expression (High vs. Low)	0.769	1.203 (0.359-4.543)

Table S3. Multiple regression analysis for factors associated with *OCT4* expression in neuroblastomas.

Factor	Standardised partial regression coefficient	*P*-value
Age	**0.119**	**0.234**
Tumor origin	**0.051**	**0.558**
INSS stage	**0.036**	**0.711**
Shimada classification	**-0.09**	**0.372**
***MYCN* amplification**	**-0.261**	**<0.05**
***TRKA* expression**	**0.026**	**0.783**
Ploidy	**-0.007**	**0.935**
***NCYM* expression**	**0.471**	**<0.05**
***MYCN* expression**	**-0.104**	**0.467**
***NANOG* expression**	**0.422**	**<0.001**
***SOX2* expression**	**0.1**	**0.314**
***KLF4* expression**	**-0.248**	**<0.05**
c-*MYC* expression	**0.244**	**<0.05**
Constant		**0.935**

Table S4. The correlation between *NCYM* and *MYCN* mRNA expression and embryonic stem cell-related genes in neuroblastomas.

mRNA expression		*NCYM* mRNA expression			*MYCN* mRNA expression		
		High *NCYM* (n=48)	Low *NCYM* (n=45)	*P*-value	High *MYCN* (n=48)	Low *MYCN* (n=45)	*P*-value
OCT4 mRNA expression	High *OCT4* (n=46)	33	13	<0.001	28	18	0.075
	Low *OCT4* (n=47)	15	32		20	27	
c-*MYC* mRNA expression	High c-*MYC* (n=46)	22	24	0.303	22	24	0.303
	Low c-*MYC* (n=47)	26	21		26	21	
KLF4 mRNA expression	High *KLF4* (n=46)	18	28	<0.05	17	29	<0.01
	Low *KLF4* (n=47)	30	17		31	16	
NANOG mRNA expression	High *NANOG* (n=46)	29	17	<0.05	27	19	0.126
	Low *NANOG* (n=47)	19	28		21	26	
SOX2 mRNA expression	High *SOX2* (n=46)	20	26	0.089	20	26	0.089
	Low *SOX2* (n=47)	28	19		28	19	

Figure S1. NCYM and MYCN induced expression of embryonic stem cell-related genes Quantitative real-time RT-PCR analyses of *NCYM*, *MYCN* and ES cell-related genes in NCYM- or MYCN-transfected SK-N-AS neuroblastoma cells. Two days after transfection, mRNA expression levels were measured by real-time RT-PCR with *β-actin* as an internal control. Triangles indicate the increasing amount of NCYM expression plasmid (0, 50, 100 and 200 ng).

Figure S2. Overexpression of c-*MYC* did not enhance the expression of *OCT4*, *NCYM* and *MYCN* in SK-N-AS human neuroblastoma cells Quantitative real-time RT-PCR analyses of *NCYM*, *MYCN* and *OCT4* in c-MYC-transfected SK-N-AS neuroblastoma cells. Forty-eight hours after transfection, mRNA expression levels were measured by real-time RT-PCR with *β-actin* as an internal control. Triangles indicate the increasing amount of c-MYC expression plasmid (0, 50, 100 and 200 ng).

Figure S3. NCYM and MYCN did not induce mouse *Oct4* in mouse neuroblastoma cells (A) Quantitative real-time RT-PCR analysis of *NCYM*, *MYCN* and ES cell-related genes in NCYM-transfected Neuro2a mouse neuroblastoma cells. Forty-eight hours after transfection, mRNA expression levels were measured by real-time RT-PCR with *β-actin* as an internal control. Triangles indicate the increasing amount of NCYM expression plasmid (0, 50, 100 and 200 ng). (B) Quantitative real-time RT-PCR analysis of *NCYM*, *MYCN* and ES cell-related genes in

MYCN-transfected Neuro2a mouse neuroblastoma cells. Forty-eight hours after transfection, mRNA expression levels were measured by real-time RT-PCR with *β-actin* as an internal control. Triangles indicate the increasing amount of MYCN expression plasmid (0, 50, 100 and 200 ng).

Figure S4. The expression of *OCT4* mRNA in tumors developed from *MYCN* and *MYCN*/*NCYM* Tg mice. Quantitative real-time RT-PCR analyses of *OCT4* in tumors of *MYCN* and *MYCN*/ *NCYM* Tg mice. mRNA expression levels were measured by real-time RT-PCR with *GAPDH* as an internal control.

Figure S5. Conservations of OCT4 binding and E-box site in *OCT4* promoter and *MYCN*/*NCYM* regions. (A) Sequences of putative E-box sites in the *OCT4* promoter in human and other species. Sequences were extracted from the UCSC genome browser on the basis of conservation. Red text indicates sequence differences compared with the human sequence. The putative E-box sites are indicated by the bold line. (B) Sequences of putative OCT4-binding sites in the *MYCN*/*NCYM* region in human and other species. Sequences were extracted from the UCSC genome browser on the basis of conservation. Red text indicates sequence differences compared with the human sequence. The putative OCT4-binding site is indicated by the bold line.

Figure S6. OCT4 induces the expression of *NCYM and MYCN* in neuroblastoma cells. (A) Quantitative real-time RT-PCR analysis of *NCYM* and *MYCN* in OCT4-transfected SK-N-AS neuroblastoma cells. Forty-eight hours after transfection, mRNA expression levels were measured by real-time RT-PCR with *β-actin* as an internal control. (B) Luciferase activity of *MYCN* and *NCYM* reporters after OCT4 transfection of SK-N-AS neuroblastoma cells. Forty-eight hours after transfection, cells were subjected to luciferase reporter assay. Data are shown as the fold change in the luciferase activity. The activities were standardized by control cells.

Figure S7. Asymmetric cell division in human neuroblastoma cells. (A) Representative images of symmetric distribution of NuMA during the late stage of mitosis in SK-N-AS (*MYCN*-non-amplified) and BE (2)-C (*MYCN*-amplified) neuroblastoma cells. Tubulin-α is indicated in red, NuMA is green and DNA is blue. Arrows show the distribution of NuMA on the cell cortex. Scale bars, 5 μm. (B) Quantification of cells with ACD in human neuroblastoma cells during late metaphase and anaphase. Error bars represent SEM from three independent experiments. Statistical significance determined by the Student's *t*-test, $*P < 0.05$.

Figure S8. Conservations of the E-box site at the *MYCN*/*NCYM* region. (A) Sequences of putative E-box sites in the *MYCN*/*NCYM* region in human and other species. Sequences were extracted from

the UCSC genome browser on the basis of conservation. Red text indicates sequence differences compared with the human sequence. The putative E-box sites are indicated by the bold line.

Table S1. Univariate Cox regression analysis using *OCT4* expression level and clinical prognosis factors in *MYCN*-amplified neuroblastomas.

Table S2. Multivariate Cox regression analysis using *OCT4* expression level and clinical prognosis factors in *MYCN*-amplified neuroblastomas.

Table S3. Multiple regression analysis for the factors associated with *OCT4* expression neuroblastomas.

Table S4. The correlation between *NCYM*, *MYCN* mRNA expression and ES cell-related genes in neuroblastoma

References

1 Cheung NK, Dyer MA. Neuroblastoma: developmental biology, cancer genomics and immunotherapy. *Nat Rev Cancer* 2013; **13**:397-411.

2 Brodeur GM, Seeger RC, Schwab M, Varmus HE, Bishop JM. Amplification of N-myc in untreated human neuroblastomas correlates with advanced disease stage. *Science* 1984; **224**:1121-4.

3 Weiss WA, Aldape K, Mohapatra G, Feuerstein BG, Bishop JM. Targeted expression of MYCN causes neuroblastoma in transgenic mice. *EMBO J* 1997; **16**:2985-95.

4 Eilers M, Eisenman RN. Myc's broad reach. *Genes Dev* 2008; **22**:2755-66.

5 Meyer N, Penn LZ. Reflecting on 25 years with MYC. *Nat Rev Cancer* 2008; **8**:976-90.

6 Suenaga Y, Islam SM, Alagu J *et al*. NCYM, a Cis-antisense gene of MYCN, encodes a de novo evolved protein that inhibits GSK3beta resulting in the stabilization of MYCN in human neuroblastomas. *PLoS Genet* 2014; **10**:e1003996.

7 Suenaga Y, Kaneko Y, Matsumoto D, Hossain MS, Ozaki T, Nakagawara A. Positive auto-regulation of MYCN in human neuroblastoma. *Biochem Biophys Res Commun* 2009; **390**:21-6.

8 Brodeur GM. Neuroblastoma: biological insights into a clinical enigma. *Nat Rev Cancer* 2003; **3**:203-16.

9 Pezzolo A, Parodi F, Marimpietri D *et al*. Oct-4+/Tenascin C+ neuroblastoma cells serve as progenitors of tumor-derived endothelial cells. *Cell Res* 2011; **21**:1470-86.

10 Molenaar JJ, Domingo-Fernandez R, Ebus ME et al. LIN28B induces neuroblastoma and enhances MYCN levels via let-7 suppression. *Nat Genet* 2012; **44**:1199-206.

11 Ross RA, Spengler BA, Domenech C, Porubcin M, Rettig WJ, Biedler JL. Human neuroblastoma I-type cells are malignant neural crest stem cells. *Cell Growth Differ* 1995; **6**:449-56.

12 Hammerle B, Yanez Y, Palanca S *et al*. Targeting neuroblastoma stem cells with retinoic acid and proteasome inhibitor. *PLoS One* 2013; **8**:e76761.

13 Ohira M, Oba S, Nakamura Y *et al*. Expression profiling using a tumor-specific cDNA microarray predicts the prognosis of intermediate risk neuroblastomas. *Cancer Cell* 2005; **7**:337-50.

14 Cotterman R, Knoepfler PS. N-Myc regulates expression of pluripotency genes in neuroblastoma including lif, klf2, klf4, and lin28b. *PLoS One* 2009; **4**:e5799.

15 Niwa H. How is pluripotency determined and maintained? *Development* 2007; **134**:635-46.

16 Izumi H, Kaneko Y. Evidence of asymmetric cell division and centrosome inheritance in human neuroblastoma cells. *Proc Natl Acad Sci U S A* 2012; **109**:18048-53.

17 Westermann F, Muth D, Benner A *et al.* Distinct transcriptional MYCN/c-MYC activities are associated with spontaneous regression or malignant progression in neuroblastomas. *Genome Biol* 2008; **9**:R150.

18 Shum CK, Lau ST, Tsoi LL *et al.* Kruppel-like factor 4 (KLF4) suppresses neuroblastoma cell growth and determines non-tumorigenic lineage differentiation. *Oncogene* 2013; **32**:4086-99.

19 Kim J, Woo AJ, Chu J *et al.* A Myc network accounts for similarities between embryonic stem and cancer cell transcription programs. *Cell* 2010; **143**:313-24.

20 Young RA. Control of the embryonic stem cell state. *Cell* 2011; **144**:940-54.

21 Chambers I, Colby D, Robertson M *et al.* Functional expression cloning of Nanog, a pluripotency sustaining factor in embryonic stem cells. *Cell* 2003; **113**:643-55.

22 Matthay KK, Villablanca JG, Seeger RC *et al.* Treatment of high-risk neuroblastoma with intensive chemotherapy, radiotherapy, autologous bone marrow transplantation, and 13-cis-retinoic acid. Children's Cancer Group. *N Engl J Med* 1999; **341**:1165-73.

23 Boyer LA, Lee TI, Cole MF *et al.* Core transcriptional regulatory circuitry in human embryonic stem cells. *Cell* 2005; **122**:947-56.

24 Nakagawa M, Koyanagi M, Tanabe K *et al.* Generation of induced pluripotent stem cells without Myc from mouse and human fibroblasts. *Nat Biotechnol* 2008; **26**:101-6.

25 Kotkamp K, Kur E, Wendik B *et al.* Pou5f1/Oct4 promotes cell survival via direct activation of mych expression during zebrafish gastrulation. *PLoS One* 2014; **9**:e92356.

26 Chen S, Zhang YE, Long M. New genes in Drosophila quickly become essential. *Science* 2010; **330**:1682-5.

27 Reinhardt JA, Wanjiru BM, Brant AT, Saelao P, Begun DJ, Jones CD. De novo ORFs in Drosophila are important to organismal fitness and evolved rapidly from previously non-coding sequences. *PLoS Genet* 2013; **9**:e1003860.

Source of Support

This work was supported in part by a Grant-in-Aid from the Ministry of Health, Labour and Welfare for the Third Term Comprehensive Control Research for Cancer, Japan (AN), a Grant-in-Aid from the Project for Development of Innovative Research on Cancer Therapeutics (P-Direct),Ministry of Education, Culture, Sports, Science and Technology, Japan (AN), a Grant-in-Aid from Takeda Science Foundation (AN), a Grant-in-Aid for Scientific Research on Priority Areas (JSPS KAKENHI Grant Number 17015046) (AN), a Grant-in-Aid for Scientific Research (A) (JSPS KAKENHI Grant Number 24249061) (AN), a Fund for Health and labor Sciences Research (Grant Number 26271201) (AN), a Grant-in-Aid for Research Activity start-up (JSPS KAKENHI Grant Number 22890241) (YS) and a Grant-in-Aid for Young Scientists (B) (JSPS KAKENHI Grant Number 24700957) (YS) from the Japan Society for the Promotion of Science (JSPS).

Acknowledgments

First, I would like to appreciate Dr. Masatoshi Tagawa, who provided me with the opportunity to finish my Ph.D. course and the previous supervisor, Dr. Akira Nakagawara, for excellent guidance in the field of molecular biology of cancer and the opportunity of my Ph.D. research under his supervision.

Yusuke Suenaga Ph.D. also deserves special appreciation, in particular, for guidance and support to critical evaluation of my research, experimental design and helpful scientific direction.

I need to thank all the students and staffs in Chiba Cancer Center Research Institute for their helpful discussion, advice, and assistance to my research.

Finally, I want to thank my parents for supporting me to finish my Ph.D. degree course. Thank you very much.

Cancer Science
2015 年 1 月投稿中